Research Square

Preprints are preliminary reports that have not undergone peer review.
They should not be considered conclusive, used to inform clinical practice,
or referenced by the media as validated information.

Magnetic Signatures and Geochemical Fingerprints of Heavy-Mineral Black Sands Along the Bayelsa Coast, Niger Delta

Francis Omonefe

francisoo@fuotuoke.edu.ng

Federal University Otuoke

Edeye Ejaita

Niger Delta University

Christopher Unyime Ebong

Zirconex Mining and Metal Laboratory

Research Article

Keywords: aeromagnetics, black sand, coastal placer, heavy minerals, ilmenite, Niger Delta, structural complexity, zircon

Posted Date: September 1st, 2026

DOI: https://doi.org/10.21203/rs.3.rs-10745621/v1

License: This work is licensed under a Creative Commons Attribution 4.0 International License.
Read Full License

Additional Declarations: No competing interests reported.

MAGNETIC SIGNATURES AND GEOCHEMICAL FINGERPRINTS OF HEAVY-MINERAL BLACK SANDS ALONG THE BAYELSA COAST, NIGER DELTA

Francis Omonefe[1]*, Edeye Ejaita[2], Christopher Unyime Ebong[3]

[1] Department of Geology, Federal University Otuoke, Bayelsa State, Nigeria
[2]Department of Physics, Niger Delta University, Wilberforce Island, Amassoma, Bayelsa State, Nigeria
[3]Zirconex Mining and Metal Laboratory, Abuja, Nigeria
Correspondence: francisoo@fuotuoke.edu.ng
ORCID: Francis Omonefe 0000-0001-8551-4585; Edeye Ejaita 0009-0009-4698-5750

Abstract

Heavy-mineral black sands along the Bayelsa coast of the Niger Delta were investigated using aeromagnetic, geological, field and geochemical data to assess their magnetic expression and mineralogical significance. Aeromagnetic data acquired at a nominal terrain clearance of 80 m and 500 m flight-line spacing were processed to generate total magnetic intensity (TMI), regional, residual, reduction-to-equator and first vertical derivative maps. The TMI field ranges from approximately −115.4 to −8.4 nT, while the residual field ranges from −52.4 to +31.5 nT. Broad regional anomalies dominate the inland and offshore sectors, whereas shorter-wavelength magnetic variations occur along the Akassa – Brass - eastern coastal corridor, where the black-sand sampling sites are located. First vertical derivative and lineament analyses further emphasise shallow magnetic heterogeneity along this coastal zone. Structural-complexity highs and the integrated structural-anomaly polygons overlap or lie close to the three field-confirmed black-sand sites. Field observations confirmed unconsolidated dark-grey to black sand concentrations within the modern beach environment. Geochemical analysis of a representative sample yielded 34.112 wt% SiO_2, 30.031 wt% ZrO_2, 14.790 wt% Fe_2O_3 and 14.412 wt% TiO_2, defining a pronounced Zr–Ti–Fe geochemical fingerprint. The magnetic anomalies are interpreted to reflect mainly Fe-bearing heavy minerals, including Fe – Ti oxides, whereas zircon enrichment is principally indicated by the high ZrO_2 content. The coincidence of shallow magnetic variability, favourable coastal depositional conditions and geochemical enrichment supports the presence of a heavy-mineral placer system. Further systematic sampling, ground magnetic surveys and mineralogical analyses are required to establish deposit continuity, mineral proportions and economic potential.

Keywords: aeromagnetics; black sand; coastal placer; heavy minerals; ilmenite; Niger Delta; structural complexity; zircon

1 INTRODUCTION

Coastal heavy-mineral sands are placer accumulations formed when minerals of relatively high density are hydraulically concentrated within beaches, barrier systems, dunes, tidal inlets and shallow-marine environments (Dill et al., 2021). Economically important components include

ilmenite, rutile and leucoxene as titanium feedstocks, together with zircon, monazite, garnet and magnetite (Raju, 2025). Repeated weathering, fluvial delivery and coastal reworking separate grains according to density, size and shape, producing dark heavy-mineral-rich laminae, lenses and lag concentrations within otherwise quartz-rich sand (Surour & El-Tohamy, 2024; Griffioen et al., 2016).

Magnetic and geochemical observations respond to different parts of this mineral assemblage and are therefore complementary (Carrero et al., 2022). Magnetite and Fe-bearing titanium oxides can generate measurable magnetic responses, whereas zircon contributes little directly to bulk magnetic susceptibility (Liu et al., 2012). Magnetic mapping can consequently identify zones of enhanced magnetic-mineral concentration, while bulk geochemistry can test whether Fe, Ti and Zr are enriched in field samples. Recent coastal placer studies likewise show that mineral separation, XRD and SEM-EDX are ultimately required to convert bulk chemical enrichment into defensible mineral proportions (Trujillo et al., 2022; Ahmed et al. 2023; Hossain et al. 2024).

The Niger Delta is an appropriate setting in which to test this integrated approach. It comprises a thick Cenozoic clastic succession overlain by extensive Quaternary deltaic and coastal deposits (Ezeh & Bhattacharya, 2023). The modern coast contains distributary channels, tidal creeks, estuaries, beaches and barrier systems that are repeatedly modified by fluvial, tidal and wave processes (Allen 1965; Short and Stauble 1967; Doust and Omatsola 1990; Obaje 2009). At Okpoama-Brass, beach sediments are dominated by fine- to medium-grained sand transported by saltation, traction and suspension, conditions compatible with hydraulic sorting of dense minerals (Akpofure and Akana 2019).

Dark beach sand alone, however, does not establish either mineral composition or economic significance, and regional airborne magnetic anomalies can be produced by sources much deeper than surficial placer sediment (Aziz et al., 2020). A useful reconnaissance model must therefore

separate broad regional magnetic components from shorter-wavelength responses, identify the spatial organization of shallow magnetic heterogeneity, and then compare the magnetic targets with field and geochemical evidence.

This study evaluates the Bayelsa coastal black sands using aeromagnetic, geological, field and geochemical data. The specific objectives are to: characterize the regional and shallow magnetic anomaly patterns; map magnetic lineaments and structural complexity; reinterpret the structural-complexity and integrated structural-anomaly zones as Ti-Fe accumulation/prospectivity regions where they coincide with the coastal black-sand system; and test that interpretation using the available black-sand geochemistry. The working hypothesis is that a magnetically defined Ti-Fe accumulation target should be supported by elevated Fe_2O_3 and TiO_2 in a representative black-sand sample, whereas ZrO_2 enrichment should provide independent evidence for a co-concentrated zirconium-bearing phase rather than a direct magnetic response.

2 GEOLOGICAL AND GEOMORPHOLOGICAL SETTING

Regional geology of the Niger Delta

The Niger Delta occupies the continental margin of the Gulf of Guinea and is one of the world's major Cenozoic clastic delta systems (Francis et al., 2026; George et al., 2019). The study area lies in southern Bayelsa State and covers the Brass-Nembe coastal sector of the Niger Delta, southwestern Nigeria (Fig. 1). Its position near the Atlantic margin places it within an active fluvial-tidal-marine depositional system in which sediment supplied from the continental hinterland is redistributed by distributary channels, tidal currents, waves and longshore transport (Macquen & Omonefe, 2026).

The regional subsurface stratigraphy comprises, from base to top, the predominantly marine-shale Akata Formation, the paralic interbedded sand-shale Agbada Formation and the continental sand-dominated Benin Formation (Short and Stauble 1967; Doust and Omatsola 1990; Tuttle et al. 1999).

For the present placer investigation, however, the most relevant materials are the much younger unconsolidated sediments of the modern deltaic and coastal plain. Late Quaternary evolution generated distributary channels, tidal creeks, mangrove swamps, estuaries, tidal flats, beach ridges, barriers and shallow-marine environments (Woodroffe, 2000). Repeated erosion, transport and redeposition provide a mechanism for sediment recycling and hydraulic concentration of dense detrital minerals (Richard et al., 2025; Allen 1965; Obaje 2009).

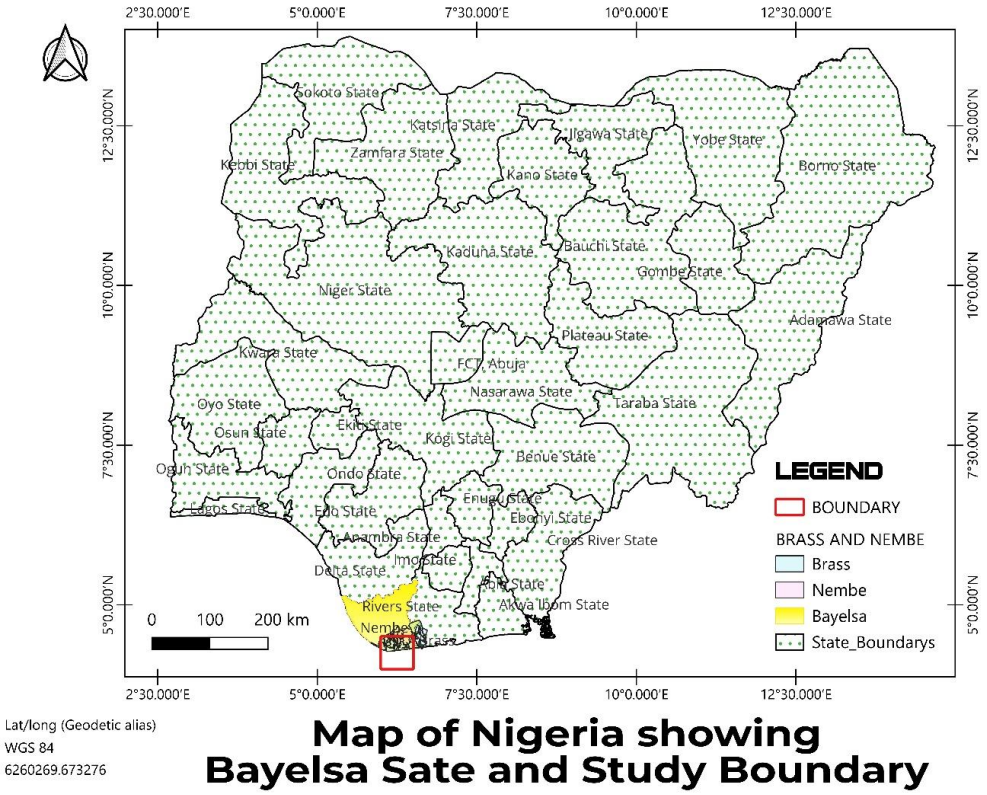


Fig. 1 Regional setting of the Brass-Nembe coastal study area. The map locates Bayelsa State and the study boundary within southern Nigeria.

Bayelsa coastal setting

The investigated area extends approximately from 6°00'E to 6°30'E and 4°00'N to 4°30'N, encompassing the Akassa-Brass-Nembe coastal corridor and the adjoining offshore sector. Macquen and Omonefe (2026) states that the terrain is low-lying and dissected by distributary channels, tidal creeks and estuarine waterways. Near-surface lithostratigraphy is dominated by unconsolidated

alluvial and coastal sediments (Fig. 2). These young deposits constitute the host material for the investigated black-sand concentrations. The dense network of distributary and tidal channels indicates strong coupling between fluvial sediment supply and marine reworking (Ejaita & Omonefe, 2026; Syvitski et al., 2005). Repeated erosion and redeposition can separate grains by density, size and hydraulic equivalence, progressively concentrating ilmenite, magnetite, rutile, zircon and other heavy minerals within beach and nearshore sediment.

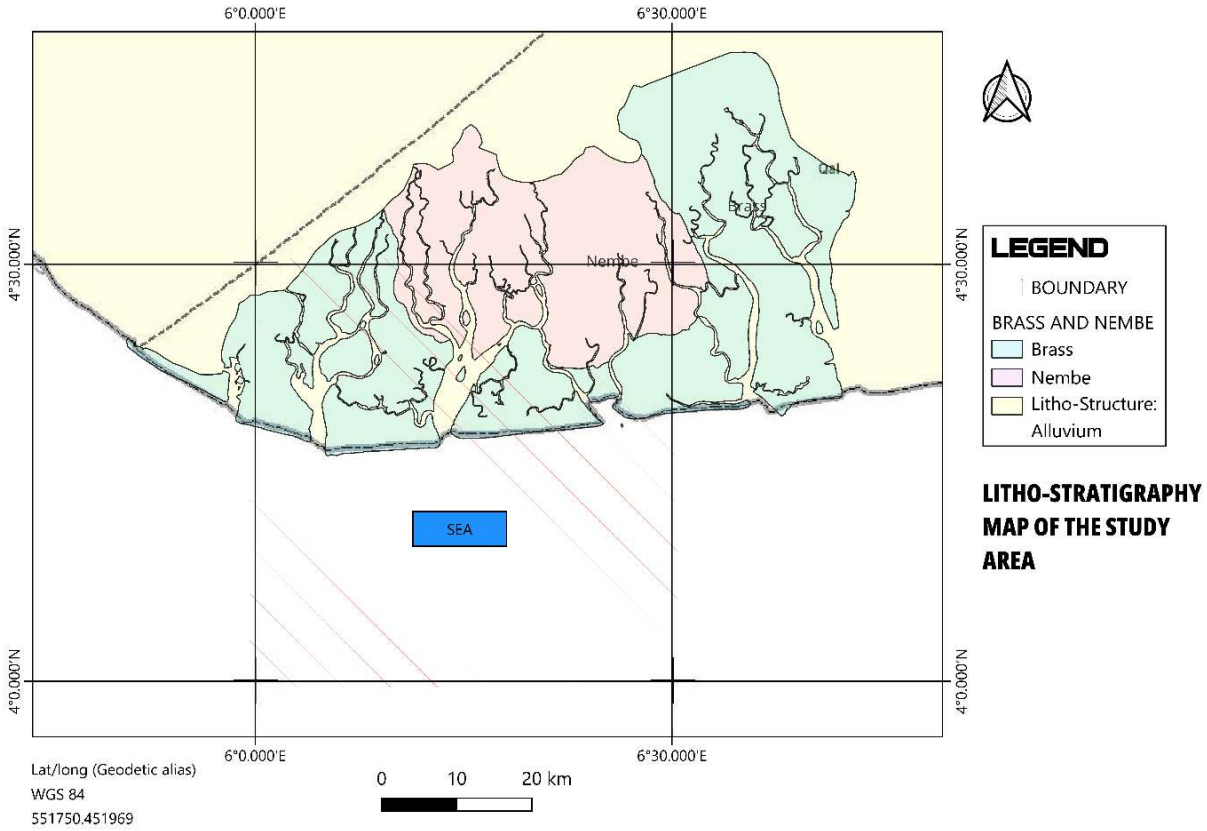


Fig. 2 Lithostratigraphic setting of the Brass-Nembe coastal sector. Unconsolidated alluvial/coastal deposits and distributary-tidal networks dominate the near-surface study area.

The broader geological compilation likewise emphasizes sandy, unconsolidated deposits along the coastal margin (Fig. 3). Field observations are consistent with a placer model: dark grey to black mineral-rich sand occurs locally at the surface and in shallow excavations and is interlayered with

lighter quartz-rich beach sand. This geometry favours repeated coastal sorting and concentration rather than emplacement as a massive bedrock-derived body (Carvalho & Woodroffe, 2023; Nanson et al., 2026).

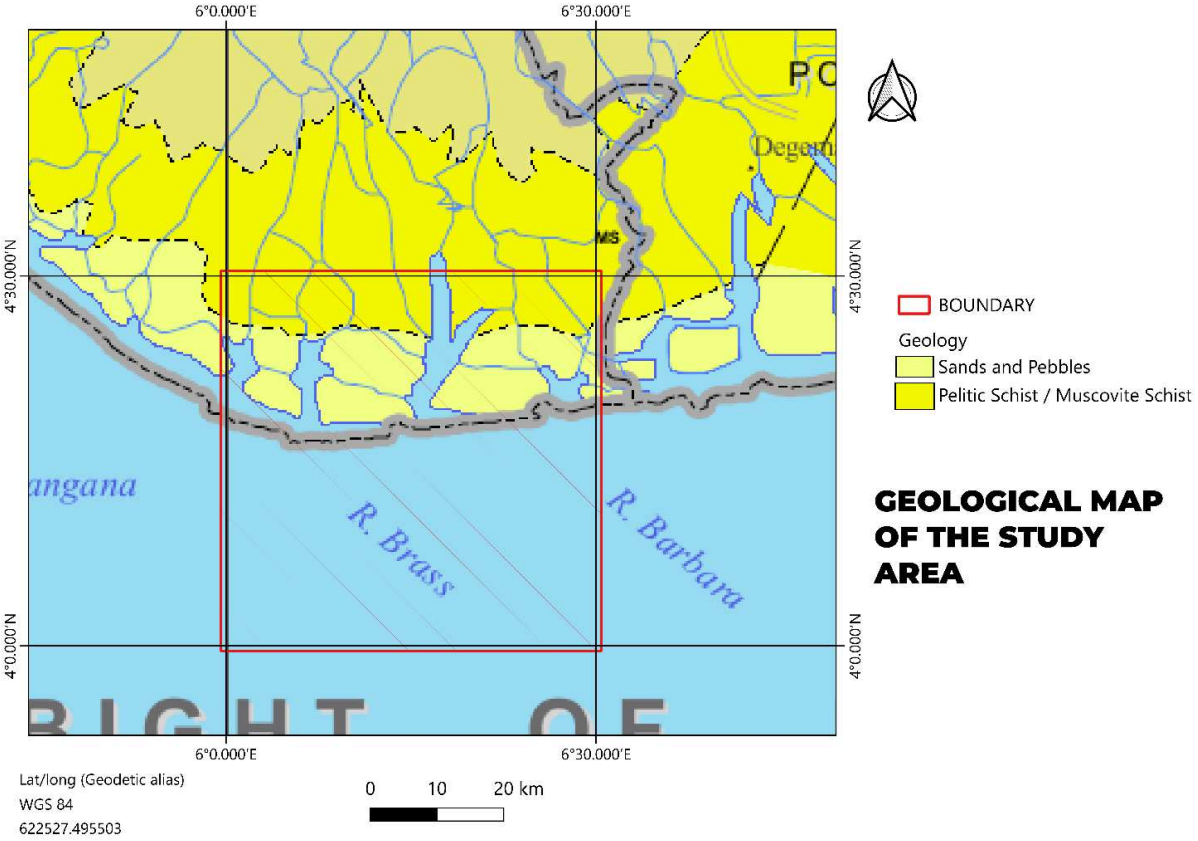


Fig. 3 Geological map of the Brass-Nembe coastal study area. Sandy and unconsolidated coastal units form the principal host for heavy-mineral placer accumulation.

3 MATERIALS AND METHODS

Aeromagnetic dataset

The available aeromagnetic dataset was processed in Oasis montaj version 10.7.1. Acquisition and delivered-grid specifications supplied with the dataset are summarized in Table 1. The delivered TMI grid has a 50 m cell size and values ranging from approximately -115.4 to -8.4 nT.

125 Table 1 Aeromagnetic survey and grid specifications.

Parameter	Specification
Magnetic recording interval	<= 0.1 s (approximately 7 m)
Mean terrain clearance	80 m
Flight-line spacing	500 m
Tie-line spacing	5,000 m
Flight-line direction	135°
Tie-line direction	45°
Magnetometer	3 x Scintrex CS3 cesium-vapour sensors
Acquisition system	FASDAS
Radar altimeter	King KR405/KR405B
Barometric altimeter	Enviro Baro/Digiquartz
Navigation	NovAtel 3151R / Omnistar RTDGPS
Flight-path processing	Real-time differential GPS
Delivered grid-cell size	50 m

126

127 **Magnetic processing**

128 Processing was designed to distinguish broad regional magnetic variation from shorter-wavelength
129 features of comparatively shallow origin. A smooth regional component was removed from the TMI
130 anomaly using the trend-removal workflow in Oasis montaj. The residual anomaly was defined as:

131 $$T_{res} = T_{TMI} - T_{regional} \quad (1)$$

132 where (T_{res}) is the residual magnetic anomaly, (T_{TMI}) is the input magnetic-anomaly field and
133 ($T_{regional}$) is the estimated regional component.

134 Because the study area lies at low geomagnetic latitude, a reduction-to-equator (RTE)
135 transformation was applied to improve the spatial association between anomaly patterns and their
136 causative sources. A first vertical derivative (FVD) grid was also generated to enhance high-
137 frequency responses and magnetic boundaries associated with comparatively shallow sources.

Derivative products can amplify acquisition or processing noise and were therefore interpreted together with the unfiltered and regional-separated fields rather than in isolation (Ejaita et al., 2025; Blakely 1995; Verduzco et al. 2004).

Magnetic lineaments, structural complexity and target mapping

Magnetic lineaments were interpreted from the processed magnetic products to summarize the spatial organization of short-wavelength boundaries and discontinuities. The resulting lineament framework was used to generate the structural-complexity surface and the integrated structural-anomaly map supplied with the magnetic study. These products were compared with the coastal geomorphology and sampling locations to define reconnaissance target zones. Because the host environment is unconsolidated coastal sediment and the target minerals are Fe-bearing heavy-mineral phases, the high-complexity zones and polygonal structural anomalies are evaluated in this paper as interpreted Ti-Fe accumulation/prospectivity regions. The mapping remains an indirect magnetic interpretation and does not by itself identify mineral species, grade or deposit thickness.

Field investigation and sampling

Field reconnaissance focused on the coastal sector where dark heavy-mineral-rich sands were exposed. Three bulk beach-sand locations were documented (Table 2). Location 1 was sampled from a shallow excavation to approximately 1 m depth, whereas Locations 2 and 3 were sampled at the surface. At each site, the colour, unconsolidated character and relationship between dark and light sand fractions were visually examined. Representative field evidence and sample appearance are shown in Fig. 4.

Table 2 Black-sand sampling locations.

Sample	Longitude (°E)	Latitude (°N)	Depth	Material

Location 1	6.050811	4.290034	~1 m	Bulk beach sand
Location 2	6.290140	4.293309	Surface	Bulk beach sand
Location 3	6.412777	4.305805	Surface	Bulk beach sand

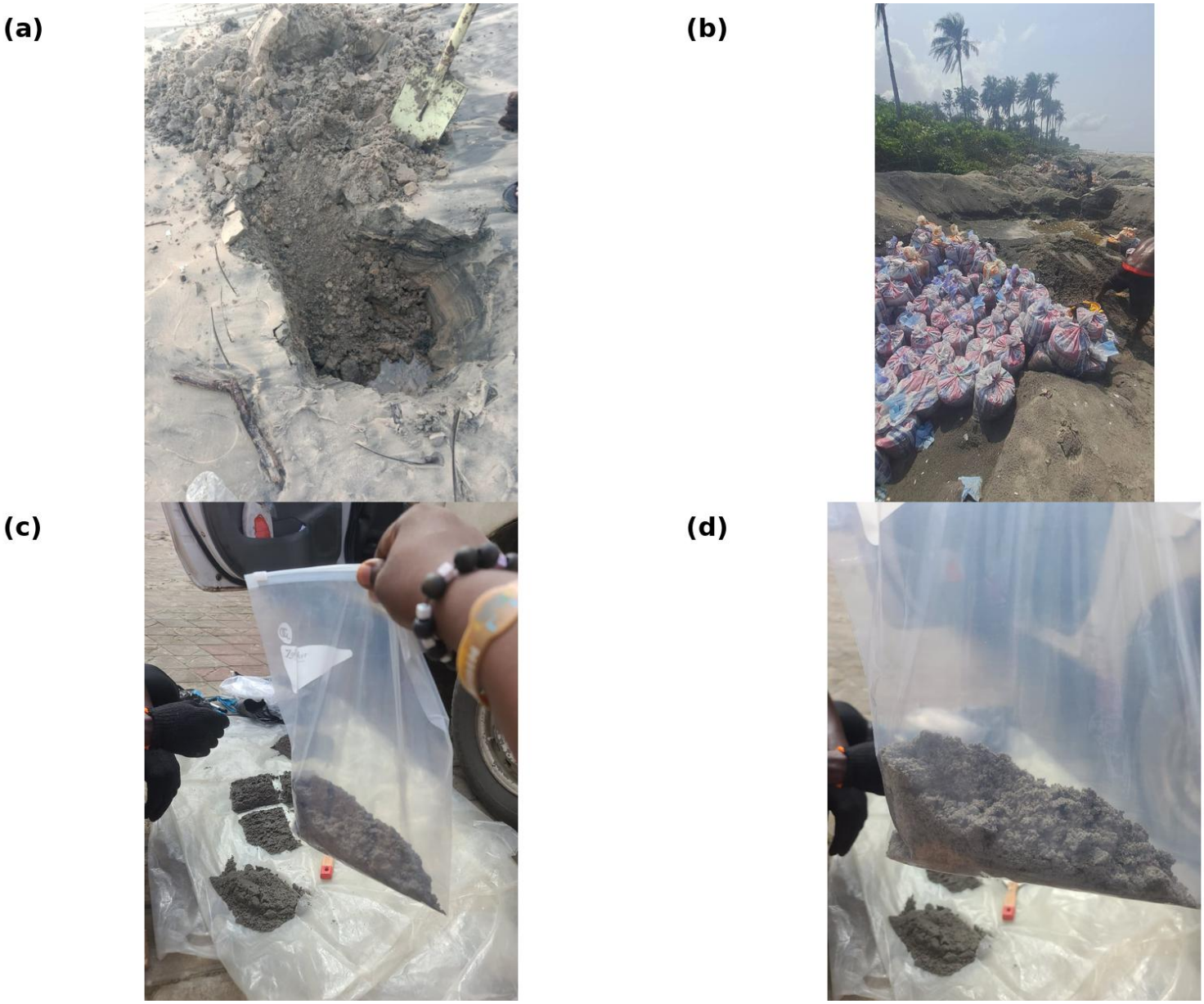


Fig. 4 Representative field occurrence and black-sand sample material. (a) Shallow excavation at Location 1; (b) collected bulk beach sand at Location 2; (c) representative black-sand specimen from Location 1; (d) packaged black-sand sample.

Geochemical analysis

A representative black-sand specimen from Location 1 was submitted for an ilmenite/multi-element assay. The analytical programme used atomic absorption spectrometry (AAS), colorimetry,

169 gravimetry and titrimetry with reference to laboratory ASTM procedures, ISO/IEC 17025
170 requirements and internal standard operating procedures. The requested suite included Al, As, Ba,
171 Ca, Cd, Cr, Cu, Co, Fe_2O_3, Ga, Ge, K, Mg, Mn, Mo, Ni, P, Pb, SiO_2, S, Sb, TiO_2, Sn, V, Zn and
172 ZrO_2. Only the reported quantified values are tabulated in the Results.

173 **Geochemical indices and mineral-equivalent calculations**

174 Two simple oxide ratios were calculated to characterise the Fe–Ti–Zr association:

175 $$R_{Ti/Fe} = \frac{TiO_2}{Fe_2O_3} \quad (2)$$

176 and

177 $$R_{Zr/Ti} = \frac{ZrO_2}{TiO_2} \quad (3)$$

178 Zircon-equivalent and ilmenite-equivalent contents were calculated by assigning all measured ZrO_2
179 to stoichiometric zircon ($ZrSiO_4$) and all measured TiO_2 to ideal ilmenite ($FeTiO_3$). These values
180 are theoretical mineral equivalents, not certified mineral grades, because bulk chemistry cannot
181 uniquely identify the host phase of Ti or Zr.

182

183 # 4 RESULTS

184 **Total magnetic intensity**

185 The TMI anomaly ranges from approximately -115.4 to -8.4 nT and displays a marked north-south
186 magnetic contrast (Fig. 5). Relatively higher responses dominate the northern part of the study area,
187 whereas lower values occur across the central and southwestern offshore sectors. A broad west-east
188 magnetic high characterizes the north, while the offshore area is dominated by a broad magnetic
189 low.

190 For black-sand exploration, the most relevant feature is the Akassa-Brass-eastern coastal corridor,
191 where shorter-wavelength magnetic variations are superimposed on the regional field. The sampling

locations lie within or close to this coastal magnetic-gradient zone. The TMI pattern is therefore treated as reconnaissance evidence of magnetic heterogeneity rather than direct confirmation of mineralized sand.

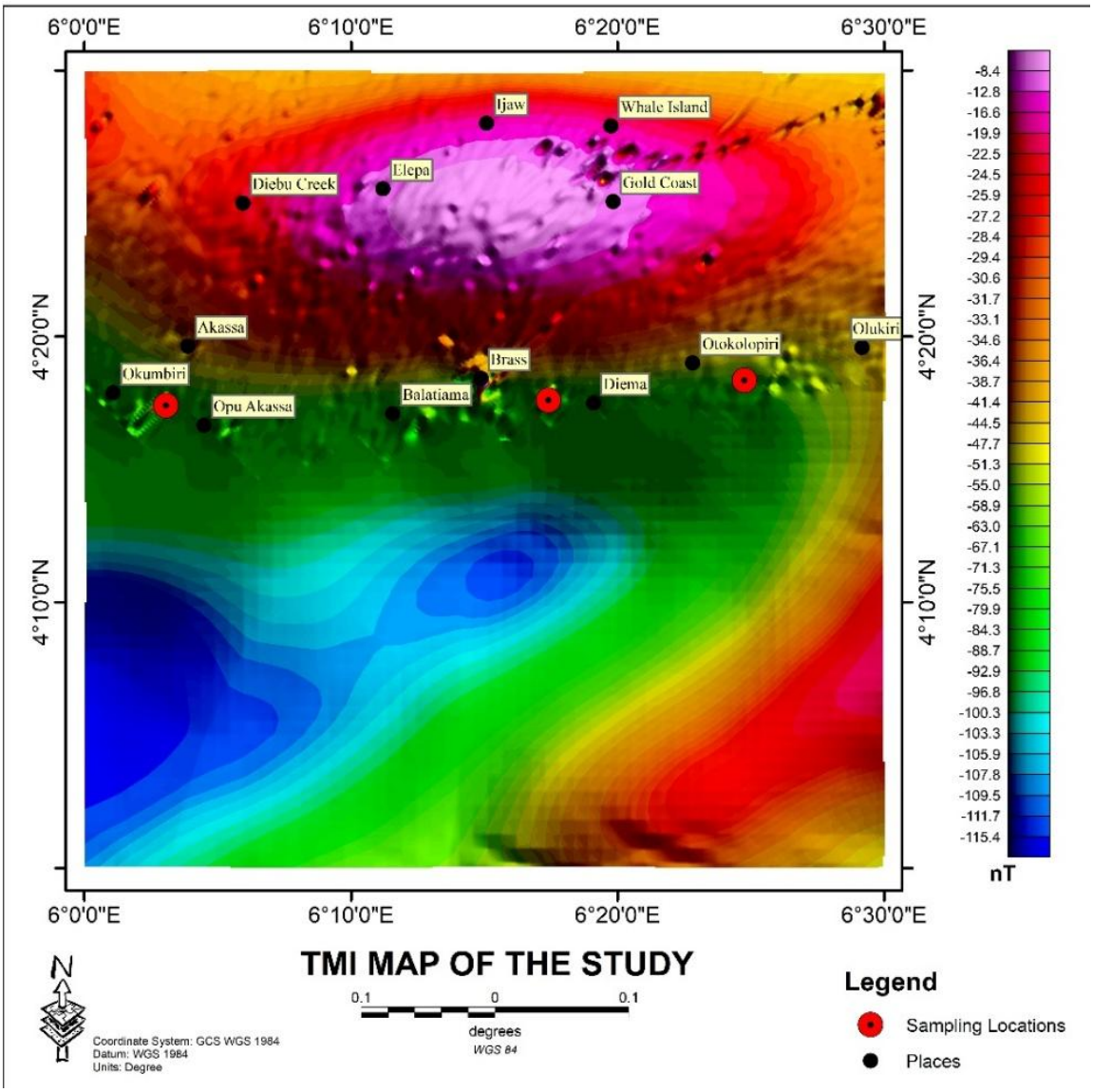


Fig. 5 Total magnetic intensity anomaly and black-sand sampling sites. TMI values range from approximately -115.4 to -8.4 nT; shorter-wavelength variability is evident along the coastal corridor.

Regional and residual magnetic fields

The regional magnetic field ranges from approximately -76.3 to -23.4 nT and increases smoothly towards the northeast (Fig. 6). Its long-wavelength character is consistent with a regional magnetic source and was treated as background for the shallow-target interpretation. Removal of this

component produced a residual field ranging from approximately -52.4 to +31.5 nT. The residual grid is not reproduced here, but it was used together with the derivative products to distinguish local magnetic variability from the broad regional trend.

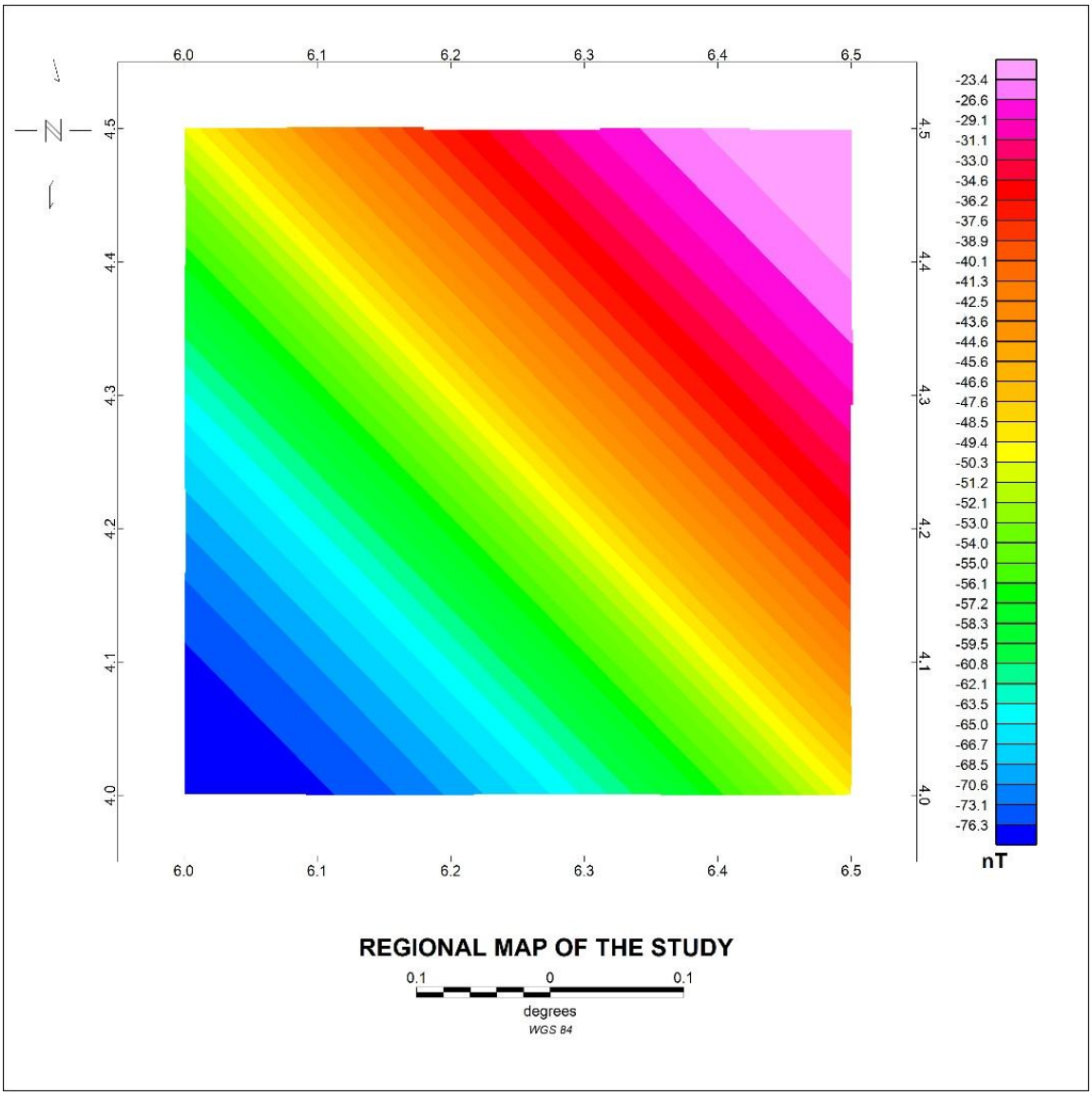


Fig. 6 Regional magnetic anomaly of the study area. The smooth long-wavelength component ranges from approximately -76.3 to -23.4 nT.

4.3 Reduction-to-equator magnetic anomaly

The RTE magnetic field ranges from approximately -108.7 to -13.2 nT and retains the principal regional anomaly domains while modifying anomaly position for the low-latitude geomagnetic setting (Fig. 7). Higher responses remain concentrated in the northern sector and a pronounced

magnetic low occupies the central-southwestern sector. Local short-wavelength variations persist along the coastline after transformation, supporting their use as shallow-source reconnaissance features.

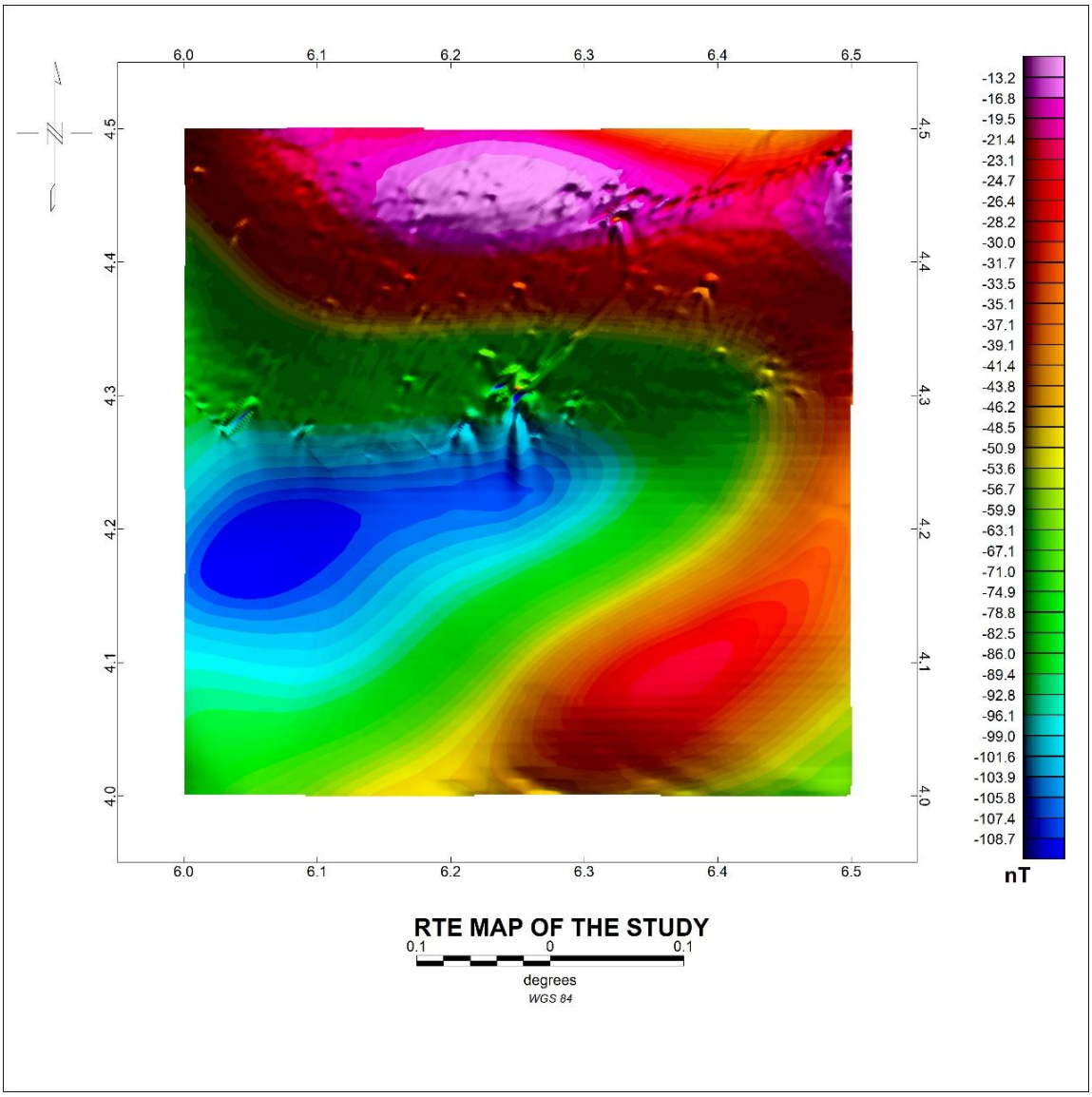


Fig. 7 Reduction-to-equator magnetic anomaly of the study area. RTE values range from approximately -108.7 to -13.2 nT; coastal short-wavelength variability remains evident.

First vertical derivative

The FVD map enhances short-wavelength magnetic responses and shallow magnetic boundaries (Fig. 8). High-frequency variations are particularly evident along the Okumbiri-Akassa-Brass-Otokolopiri coastal corridor, where the black-sand sampling sites occur near local positive-negative

derivative contrasts. The pattern indicates pronounced shallow magnetic heterogeneity relevant to Fe-bearing heavy minerals. The strongest high-frequency texture, especially in the northern sector, is interpreted cautiously because vertical derivatives can also enhance survey noise.

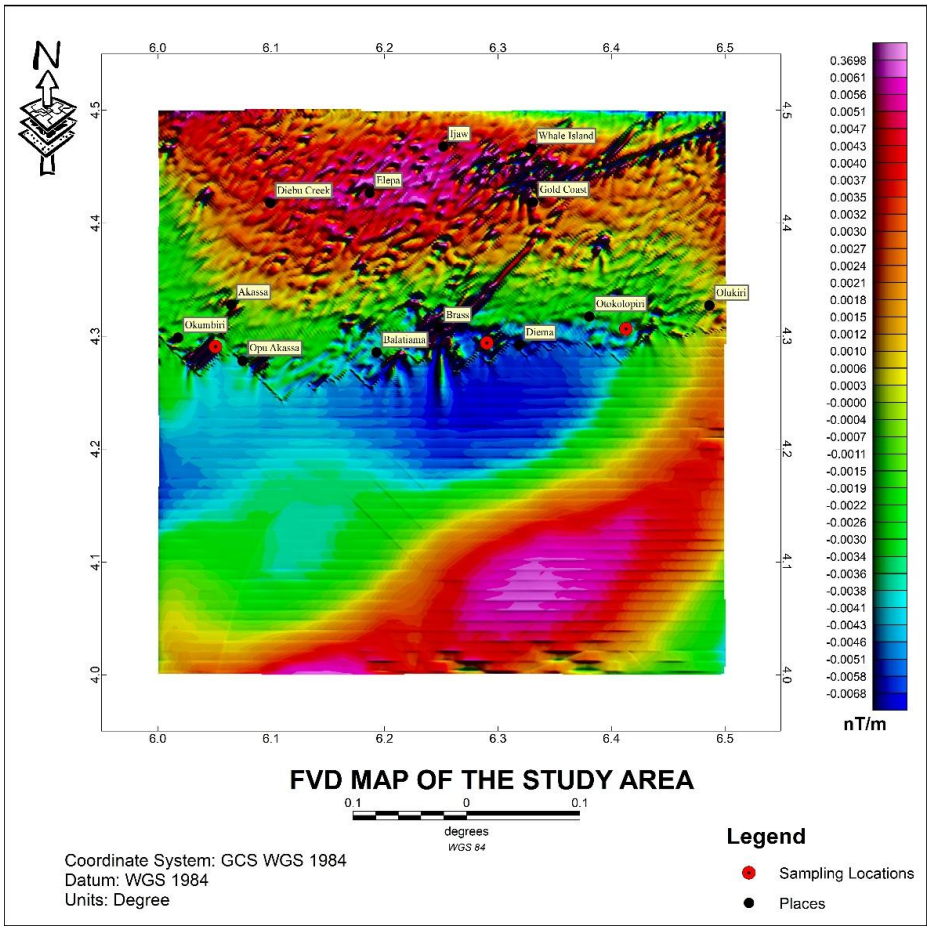
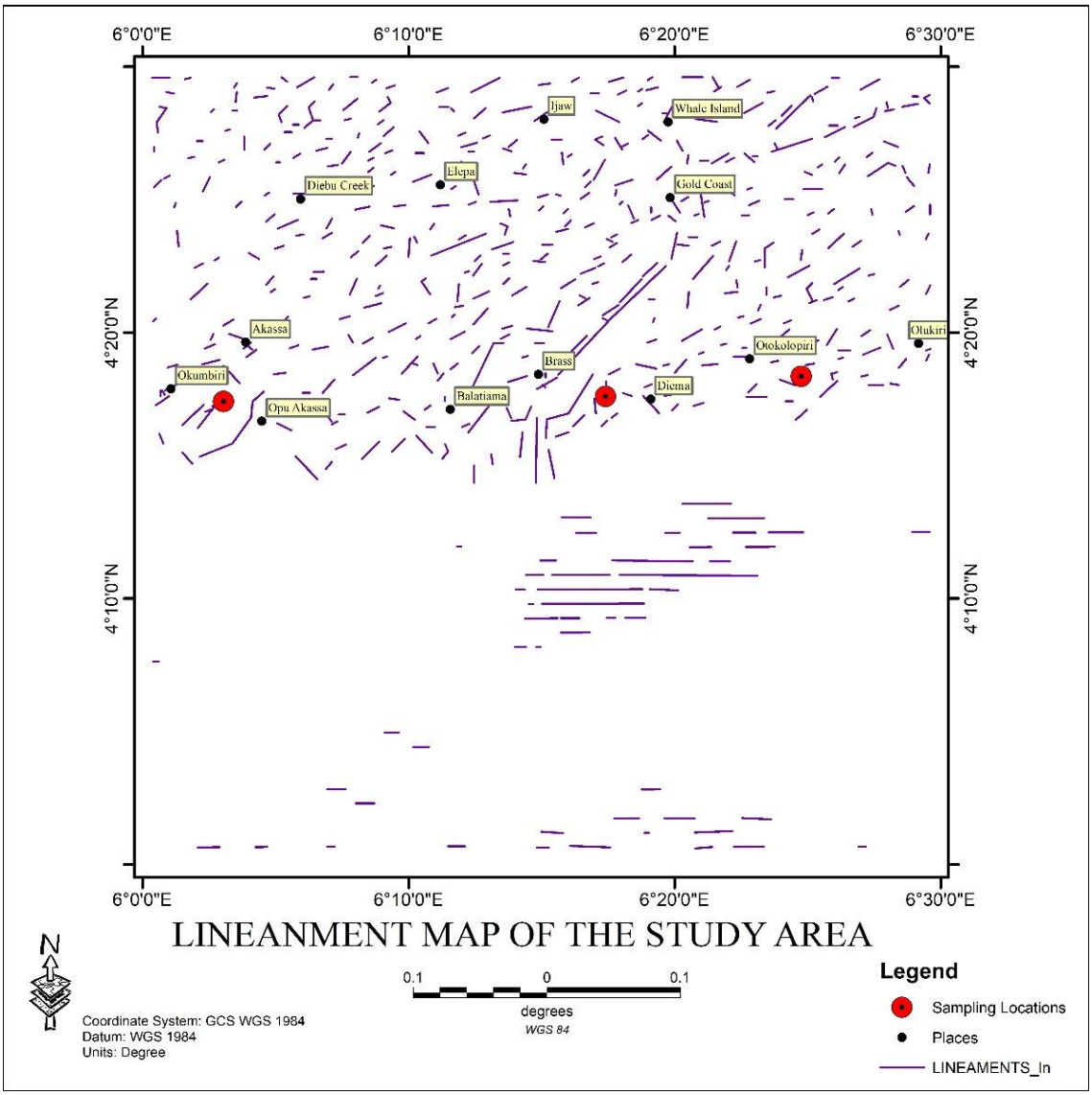


Fig. 8 First vertical derivative and black-sand sampling sites. The FVD emphasizes shallow, short-wavelength magnetic variability along the coastal target corridor.

Magnetic lineaments

Interpreted magnetic lineaments are concentrated mainly in the northern and coastal parts of the study area and show dominant NE-SW to ENE-WSW trends, with subordinate E-W, NW-SE and N-S orientations (Fig. 9). Longer NE-SW features are prominent around the Brass sector, whereas the southern offshore sector contains fewer and mainly E-W features. The lineaments are treated as magnetic boundaries or discontinuities and not automatically as confirmed faults.



234

235 Fig. 9 Interpreted magnetic lineaments and sampling sites. Dominant NE-SW to ENE-WSW trends organize the
236 coastal magnetic heterogeneity.

237 **Structural complexity and interpreted Ti-Fe accumulation regions**

238 The structural-complexity surface shows markedly higher values across the northern and coastal
239 sectors, with low values over much of the offshore area (Fig. 10). Local high-complexity zones
240 occur around Akassa, Brass and the eastern coastal corridor near the black-sand sampling locations.
241 These zones coincide with increased magnetic variability and lineament concentration.

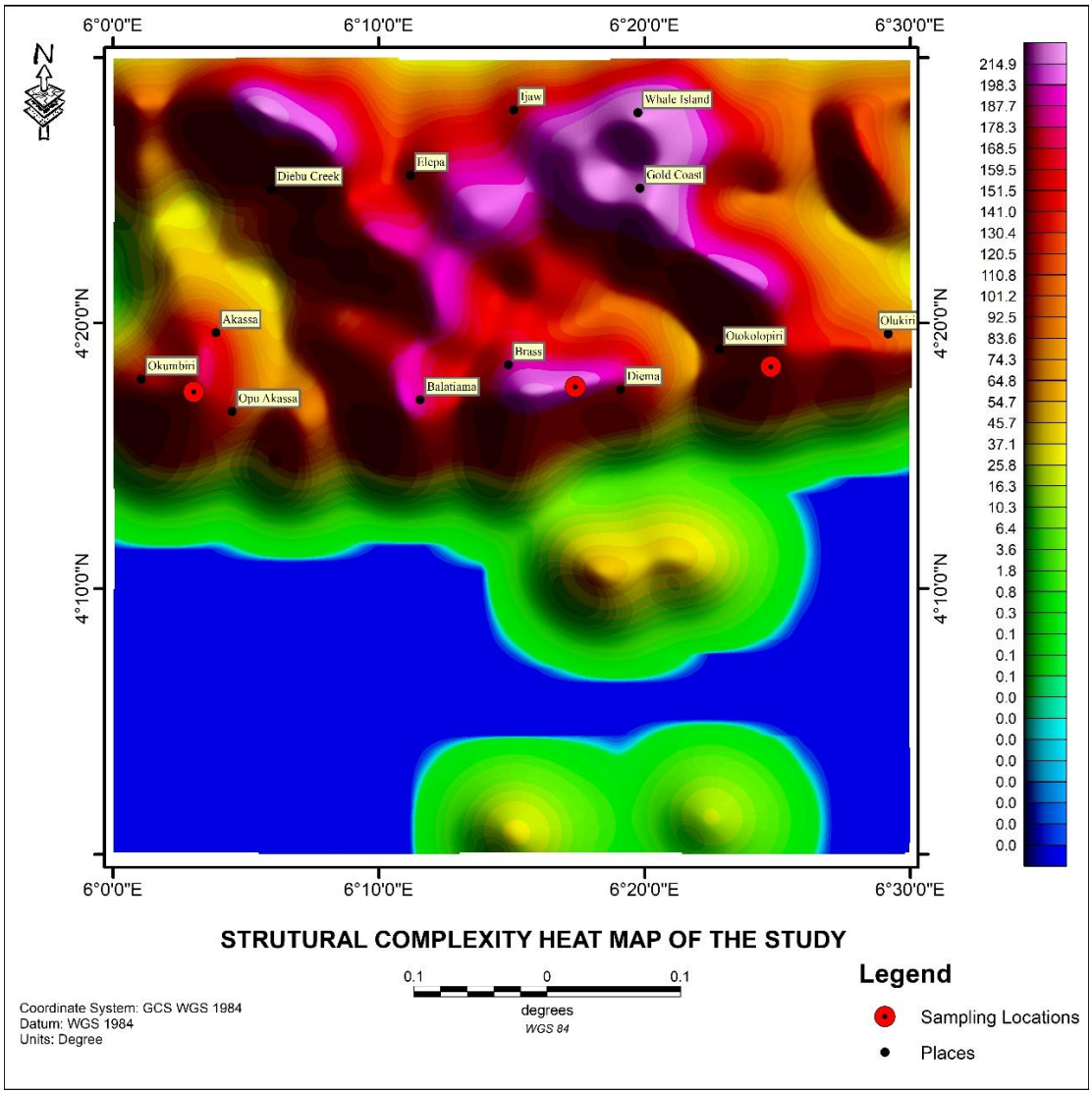


Fig. 10 Magnetic structural complexity and interpreted Ti-Fe accumulation prospectivity. Elevated complexity values cluster across the northern and coastal sectors and occur near the black-sand sampling sites.

In the context of this study, the high-complexity belt is interpreted as a Ti-Fe accumulation/prospectivity region derived from the magnetic dataset. This terminology reflects the target process being investigated: local concentration of Fe-bearing and titaniferous heavy minerals within unconsolidated coastal sediment. The interpretation is not intended to imply hydrothermal alteration or bedrock mineralization.

Integrated structural map and Ti-Fe accumulation targets

The integrated structural map contains discrete polygonal anomalies that cluster around Akassa, Balatiama, Brass, Whale Island, Gold Coast and the eastern coastal corridor (Fig. 11). The three black-sand sampling locations occur within or adjacent to some of these polygons and lineament clusters. The polygonal zones are therefore treated here as interpreted Ti-Fe accumulation targets defined by the magnetic structural analysis. Their significance is evaluated against the field and geochemical data below.

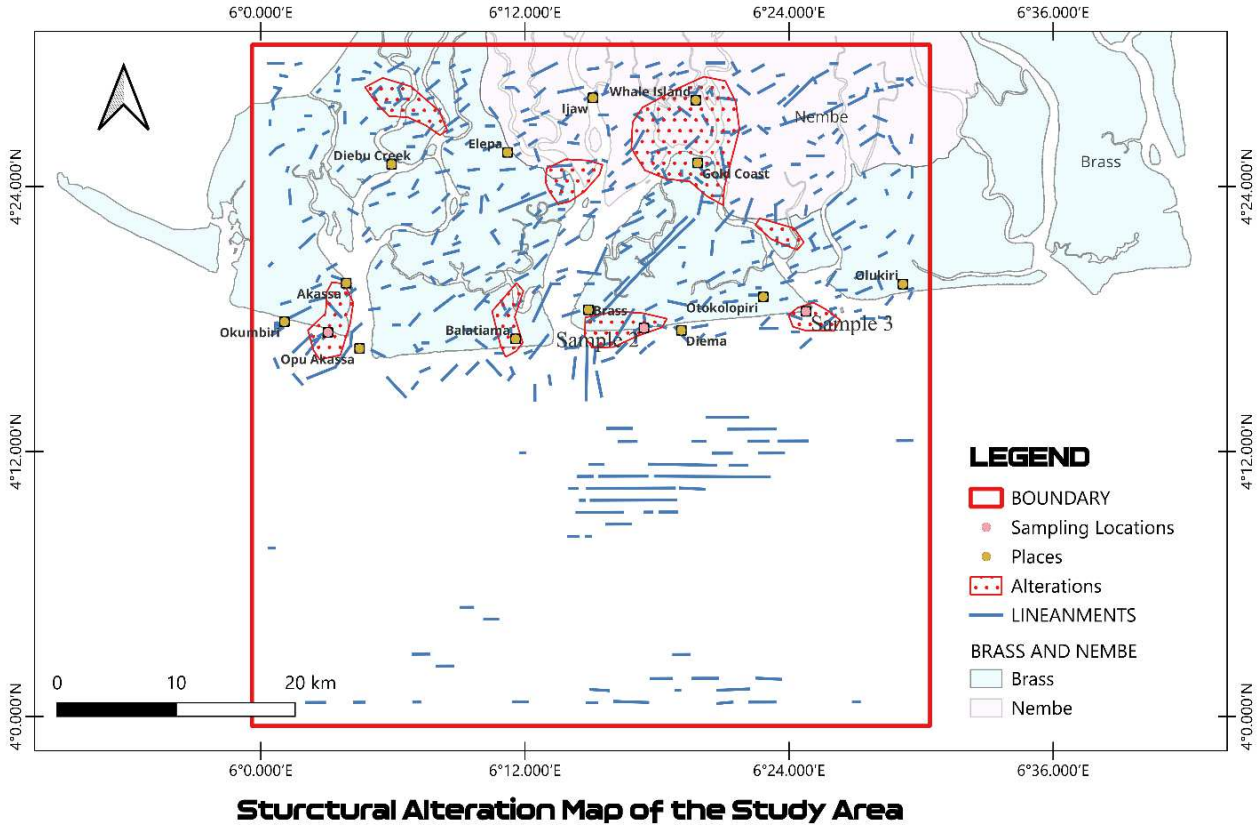


Fig. 11 Integrated magnetic structural map and interpreted Ti-Fe accumulation zones.

Field occurrence of black sands

Field observations confirm dark-grey to black unconsolidated sand within the modern Bayelsa beach environment (Fig. 4). The dark fraction occurs within lighter quartz-rich beach sand and as locally

enriched material in shallow excavations. Its granular, unconsolidated character and association with the active beach system are consistent with hydraulic sorting and placer-style concentration.

Geochemical composition and mineral-equivalent estimates

The analysed Location 1 black-sand sample is dominated by SiO_2, ZrO_2, Fe_2O_3 and TiO_2 at 34.112, 30.031, 14.790 and 14.412 wt%, respectively (Table 3). The closely comparable Fe_2O_3 and TiO_2 abundances define a strong Fe-Ti association, while the high ZrO_2 concentration demonstrates substantial enrichment of a zirconium-bearing phase.

Table 3 Major and selected trace-element composition of the Location 1 black sand.

Analyte	Concentration (wt%)
SiO_2	34.112
ZrO_2	30.031
Fe_2O_3	14.790
TiO_2	14.412
V	0.083
Mn	0.072
Ni	0.071
Al	0.062
Ca	0.037
Zn	0.035
Cu	0.016
Cr	0.011
Co	0.009
P	0.007
As	0.005
Sn	0.003

The calculated TiO_2/Fe_2O_3 ratio is 0.97 and the ZrO_2/TiO_2 ratio is 2.08. The near-unity TiO_2/Fe_2O_3 ratio supports a substantial Fe-Ti-bearing component. If all ZrO_2 is provisionally assigned to stoichiometric zircon, the sample contains approximately 44.7 wt% zircon-equivalent. If all TiO_2 is assigned to ideal ilmenite, the result is approximately 27.4 wt% ilmenite-equivalent. These are

stoichiometric equivalents only and should not be reported as measured mineral percentages until mineral phases are confirmed by XRD, SEM-EDS or quantitative mineral separation.

5 DISCUSSION

Magnetic basis for the Ti-Fe accumulation interpretation

The airborne data separate two magnetic scales that are important for placer exploration. The broad TMI and regional domains extend far beyond the modern beach and are therefore unlikely to be caused by thin surficial black-sand horizons alone. By contrast, the RTE and FVD products retain or enhance shorter-wavelength variability along the coastal corridor. Because magnetite and Fe-bearing titanium oxides are capable of contributing substantially to magnetic susceptibility, this coastal magnetic heterogeneity provides a physically plausible proxy for changes in the abundance of the magnetic heavy-mineral fraction.

The structural-complexity map and integrated structural map provide the key spatial synthesis. Their high-complexity zones and polygonal anomalies are concentrated where magnetic gradients and lineaments are dense, including sectors around Akassa and Brass and the eastern coastal corridor. In a placer setting, these features are better described as Ti-Fe accumulation/prospectivity zones than as hydrothermal alteration zones. The maps do not prove mineral identity; rather, they delineate zones in which the magnetic architecture is consistent with enhanced concentration or redistribution of Fe-bearing heavy minerals. This is the principal exploration interpretation advanced by the present study.

Geochemical corroboration of the magnetic target

The Location 1 geochemistry independently corroborates the Ti-Fe component of the magnetic interpretation. The assay contains 14.790 wt% Fe_2O_3 and 14.412 wt% TiO_2, giving a TiO_2/Fe_2O_3 ratio of 0.97. These concentrations show that the field-confirmed black sand contains a substantial Fe-Ti chemical component, consistent with the magnetic target concept. The result is particularly

relevant because the sampling locations fall within or adjacent to the coastal structural-complexity and polygonal target zones.

The term "confirmation" must nevertheless be used at the correct scale. The assay confirms Fe-Ti enrichment in the analysed Location 1 material and therefore supports the interpretation of the mapped coastal target system. It does not demonstrate that every structural-complexity high or polygon has the same composition or grade. Only one of the three field locations currently has a reported multi-element assay, so spatial continuity remains to be established.

Zr enrichment and magnetic-geochemical complementarity

The 30.031 wt% ZrO_2 concentration is a major finding but should be interpreted independently from the magnetic response. Zircon is comparatively non-magnetic, so a magnetic anomaly cannot be treated as a direct zircon anomaly. Instead, the Zr enrichment is consistent with hydraulic co-concentration of zircon with denser magnetic minerals such as magnetite and Fe-Ti oxides. The magnetic survey therefore provides a regional proxy for the magnetic fraction of the placer assemblage, while geochemistry demonstrates that the same black-sand system is also strongly enriched in a zirconium-bearing phase.

The theoretical zircon- and ilmenite-equivalent calculations illustrate the magnitude of the oxide enrichment but are not quantitative mineralogy. Natural ilmenite may deviate from ideal $FeTiO_3$ composition, Ti can occur in rutile, leucoxene or other phases, and Zr can occur outside ideal zircon. Recent coastal placer characterization demonstrates the value of combining bulk geochemistry with XRD and SEM-EDX to resolve mineral hosts and proportions (Hossain et al. 2024). The same mineralogical confirmation is required here before resource-grade statements can be made.

Coastal controls on heavy-mineral concentration

The geological and field evidence supports a placer origin for the black sands. The coastal plain is dominated by unconsolidated sediment and dissected by distributary and tidal channels (Figs. 2 and

3). Wave uprush, backwash, tidal currents and longshore transport repeatedly rework this sediment. Under suitable hydrodynamic conditions, lower-density quartz-rich grains can be preferentially removed while denser grains such as zircon, ilmenite and magnetite are retained as lag concentrations (Van Gosen et al. 2014).

The observed dark fractions occur within and beneath lighter beach sands rather than as an exposed bedrock body. This field geometry, together with the active coastal setting, favours repeated sorting and redeposition. The magnetic structural patterns may therefore reflect spatial compartments in which sediment pathways, boundaries and local hydrodynamic conditions have promoted differential accumulation of the magnetic heavy-mineral fraction, rather than tectonic structures alone.

Exploration implications and limitations

The most useful reconnaissance targets are not necessarily the strongest regional magnetic highs. Priority should instead be given to short-wavelength residual/RTE/FVD anomalies that coincide with favourable coastal geomorphology and with the structural-complexity or integrated Ti-Fe target zones. In the present dataset, the Akassa-Brass-eastern coastal corridor satisfies these criteria and contains the field-confirmed black-sand occurrences.

A practical follow-up programme should acquire high-resolution ground magnetic profiles and magnetic-susceptibility measurements across the mapped Ti-Fe targets, paired with systematic shore-parallel and shore-normal sampling. Each of the three field locations should be analysed using the same geochemical protocol, with replicates and quality-control samples. Grain-size analysis, heavy-liquid or magnetic separation, XRD and SEM-EDS should then determine mineral species and proportions.

Two limitations are fundamental. First, the 500 m airborne flight-line spacing and approximately 80 m terrain clearance are coarse relative to the likely thickness and lateral variability of individual

beach-sand lenses; the aeromagnetic products should therefore be used for reconnaissance targeting rather than direct ore-body delineation. Second, only one reported multi-element assay is available, preventing extrapolation of the Location 1 Fe-Ti-Zr composition across all mapped target zones. Future work should also archive the detailed lineament-extraction and structural-complexity parameters to maximize reproducibility of the target-mapping workflow.

6 CONCLUSIONS

This study establishes a coherent magnetic-geochemical interpretation for the Bayelsa coastal black sands. Short-wavelength magnetic variability, magnetic lineaments and structural-complexity highs define a prospective coastal belt from Akassa through Brass to the eastern study area. The structural-complexity and integrated structural-anomaly maps are interpreted as reconnaissance Ti-Fe accumulation/prospectivity maps for the coastal placer system, rather than as maps of hydrothermal alteration.

The Location 1 assay provides independent geochemical support for this interpretation, with 14.790 wt% Fe_2O_3 and 14.412 wt% TiO_2 and a TiO_2/Fe_2O_3 ratio of 0.97. The same sample contains 30.031 wt% ZrO_2, demonstrating substantial co-enrichment of a zirconium-bearing phase. The magnetic and geochemical datasets are therefore complementary: the magnetic response primarily targets Fe-bearing heavy minerals, whereas geochemistry demonstrates both Fe-Ti enrichment and the associated Zr-rich component.

The results support the presence of a Fe-Ti-Zr-bearing coastal placer system and provide a practical targeting framework for follow-up exploration. However, the current evidence is reconnaissance-scale. Ground magnetic surveying, magnetic-susceptibility measurements, systematic multi-site geochemistry, grain-size analysis, and XRD/SEM-EDS are required before continuity, thickness, mineral proportions or economic grade can be established.

List of abbreviations

AAS, atomic absorption spectrometry;

FVD, first vertical derivative;

RTE, reduction to the equator;

SEM-EDS, scanning electron microscopy-energy-dispersive X-ray spectroscopy;

TMI, total magnetic intensity;

XRD, X-ray diffraction.

Declarations

Availability of data and materials

The magnetic grids, sampling coordinates and laboratory analytical data supporting the findings of this study are available from the corresponding author on reasonable request, subject to any restrictions imposed by the original magnetic-data provider.

Competing interests

The authors declare that they have no competing interests.

Funding

The authors received no specific funding for this study.

Authors' contributions

FO conceived and designed the study, carried out the geological investigation and fieldwork, interpreted the geological and geochemical data, processed and interpreted the aeromagnetic data, carried out the magnetic and structural analyses, prepared the figures, and wrote the original draft. EE contributed to data visualization, and reviewed and edited the manuscript. CUE contributed to field sampling, sample preparation, geochemical analysis and mineralogical interpretation, and

reviewed the manuscript. All authors contributed to interpretation of the results and read and approved the final manuscript.

Acknowledgements

The authors acknowledge Frandee Consulting Service for support during field activities and Zirconex Mining and Metal Laboratory for the multi-element geochemical analysis of the black-sand sample. The authors also acknowledge the provider of the aeromagnetic dataset used in this study and the assistance of field personnel and members of the local communities during coastal reconnaissance and sample collection.

Ethics approval and consent to participate

Not applicable.

Consent for publication

Not applicable.

AI-assisted language editing

OpenAI was used to assist with English-language editing. The authors reviewed the revised text, verified the scientific content, and retain full responsibility for the data, interpretations and conclusions.

REFERENCES

Ahmed MT, Monir MU, Rajib M, Sarkar SM, Hasan Y, Quamruzzaman C, Abd Aziz A, Khan MFH, Hossain N, Hossain F, Akash FA, Shovon SM (2023) Heavy minerals identification and extraction along coastal sediments using placer mining technique. J Sediment Environ 8:81-95. doi:10.1007/s43217-022-00120-8.

Akpofure E, Akana ST (2019) Grain size analysis of sediments from Okpoama-Brass Beach in the Niger Delta. J Environ Earth Sci 9(3). doi:10.7176/JEES/9-3-09.

Allen JRL (1965) Late Quaternary Niger Delta, and adjacent areas: sedimentary environments and lithofacies. AAPG Bull 49:547-600.

Aziz A, Sief R, Ghieth B, Kaiser M (2020) Black sand deposits; their spatial distribution and hazards along the northern coast of Sinai Peninsula, Egypt. Journal of Applied Geophysics 183:104219. https://doi.org/10.1016/j.jappgeo.2020.104219.

Blakely RJ (1995) Potential theory in gravity and magnetic applications. Cambridge University Press, Cambridge.

Carrero S, Slotznick SP, Fakra SC, Sitar MC, Bone SE, Mauk JL, Manning AH, Swanson-Hysell NL, Williams KH, Banfield JF, Gilbert B (2022) Mineralogical, magnetic and geochemical data constrain the pathways and extent of weathering of mineralized sedimentary rocks. Geochimica et Cosmochimica Acta 343:180-195. https://doi.org/10.1016/j.gca.2022.11.005.

Carvalho RC, Woodroffe CD (2023) Coastal compartments: the role of sediment supply and morphodynamics in a beach management context. Journal of Coastal Conservation 27(6). https://doi.org/10.1007/s11852-023-00984-6.

Dill HG, Andrei B, Sorin-Ionut B (2021) Coastal morphology and heavy mineral accumulation in an upper-macrotidal environment - A geological-mineralogical approach from source to trap site in a natural placer laboratory (Channel Islands, Great Britain). Ore Geology Reviews 138:104311. https://doi.org/10.1016/j.oregeorev.2021.104311.

Doust H, Omatsola E (1990) Niger Delta. In: Edwards JD, Santogrossi PA (eds) Divergent/passive margin basins. AAPG Memoir 48, American Association of Petroleum Geologists, Tulsa, pp 201-238.

Ejaita E, Godwin OE, Isaac AO, Udensi EE, Omonefe F (2025) Geophysical method for determining geothermal source potential in parts of the South-West and South-South, Nigeria. Asian Journal of Research and Reviews in Physics 9(1):85-124. https://doi.org/10.9734/ajr2p/2025/v9i1184.

Ejaita E, Omonefe F (2026) Multi attribute predictions of volume of shale and porosity from seismic data over Akaso Field, Niger Delta using machine learning regression analysis. Discover Geoscience 4(1). https://doi.org/10.1007/s44288-026-00457-x.

Ezeh SC, Bhattacharya JP (2023) Quantifying a tide-dominated, wave-, and river-influenced delta in Miocene facies of the Niger Delta basin. Journal of Sedimentary Research 94(1):125-150. https://doi.org/10.2110/jsr.2023.055.

Francis O, Edeye E, Arekumo T (2026) Integrated Petrophysical Evaluation of Reservoir Quality and Hydrocarbon Potential Using Thickness-Weighted Metric from Well Logs from the Niger Delta. Research Square. https://doi.org/10.21203/rs.3.rs-9867387/v1.

George CF, Macdonald DI, Spagnolo M (2019) Deltaic sedimentary environments in the Niger Delta, Nigeria. Journal of African Earth Sciences 160:103592. https://doi.org/10.1016/j.jafrearsci.2019.103592.

Griffioen J, Klaver G, Westerhoff W (2016) The mineralogy of suspended matter, fresh and Cenozoic sediments in the fluvio-deltaic Rhine-Meuse-Scheldt-Ems area, the Netherlands: An

overview and review. Netherlands Journal of Geosciences - Geologie En Mijnbouw 95(1):23-107. https://doi.org/10.1017/njg.2015.32.

Hossain MS, Rahman MS, Taki G, Jahan M (2024) Geochemical characterization and reserve estimation of the economic heavy minerals of Sonadia Island, Bangladesh. Discov Geosci 2:65. doi:10.1007/s44288-024-00073-7.

Kumari K, Gandhi MS, Vamsi KS, et al (2020) Characterization of sedimentary environment, provenance and distribution of heavy minerals along the Tamil Nadu shoreline, east coast of India. J Sediment Environ 5:519-536. doi:10.1007/s43217-020-00030-7.

Liu Q, Roberts AP, Larrasoaña JC, Banerjee SK, Guyodo Y, Tauxe L, Oldfield F (2012) Environmental magnetism: Principles and applications. Reviews of Geophysics 50(4). https://doi.org/10.1029/2012rg000393.

Macquen BA, Omonefe F (2026) Screening-Level Deterministic Estimates of Fault-Controlled reservoir Prospects in the Mag Field, Niger Delta Basin. Journal of Engineering Research and Reports 28(7):105-121. https://doi.org/10.9734/jerr/2026/v28i71947.

Nanson R, Arosio R, Gafeira J, McNeil M, Dove D, Bjarnadóttir L, Dolan M, Post A, Nichol S, Huang Z, Guinan J, Bialik O, Webb J, Wells J, Carroll A (2026) Coastal to deep-marine geomorphic classification: A standardised framework and review of terms to support globally consistent mapping. Earth-Science Reviews 276:105439. https://doi.org/10.1016/j.earscirev.2026.105439.

Obaje NG (2009) The Niger Delta Basin. In: Geology and mineral resources of Nigeria. Lecture Notes in Earth Sciences, vol 120. Springer, Berlin, Heidelberg.

Omotoye SJ, Fadiya SL, Adesiyan TA (2016) Sedimentological study and heavy mineral analysis of sediment samples from Well-S, Niger Delta, Nigeria. Univ J Geosci 4(3):51-61. doi:10.13189/ujg.2016.040301.

Raju RD (2025) Critical Minerals-U-Th, Recoverable from the Placer Valuable Heavy Minerals in Mineral Sand Deposits. International Journal of Research and Innovation in Applied Science X(III):807-819. https://doi.org/10.51584/ijrias.2025.10030061.

Richard FO, Reuben IP, Qingzhen H, Zenghtang G, Xinbo G, Ayodele RI (2025) Heavy mineral as proxies for provenance and depositional environment in quaternary coastal alluvium in eastern Dahomey Basin, southwestern Nigeria. Discover Geoscience 3(1). https://doi.org/10.1007/s44288-025-00265-9.

Short KC, Stauble AJ (1967) Outline of geology of Niger Delta. AAPG Bull 51:761-779.

Surour AA, El-Tohamy AM (2024) Characterization of heavy minerals and their possible sources in quaternary alluvial and beach sediments by an integration of microanalytical data and spectroscopy (FTIR, RAMAN and UV-VIS). Quaternary 7(4):46. https://doi.org/10.3390/quat7040046.

493 Syvitski JP, Kettner AJ, Correggiari A, Nelson BW (2005) Distributary channels and their impact
494 on sediment dispersal. Marine Geology 222-223:75-94.
495 https://doi.org/10.1016/j.margeo.2005.06.030.

496 Trujillo W, Cobo J, Vera-Cedeño D, Palma-Cando A, Toro-Álava J, Viloria A, Ricaurte M (2022)
497 Magnetic Separation and Enrichment of Fe-Ti Oxides from Iron Titaniferous Beach Sands:
498 Process Design Applied to Coastal Ecuador. Resources 11(12):121.
499 https://doi.org/10.3390/resources11120121.

500 Tuttle MLW, Charpentier RR, Brownfield ME (1999) The Niger Delta petroleum system: Niger
501 Delta Province, Nigeria, Cameroon, and Equatorial Guinea, Africa. U.S. Geological Survey
502 Open-File Report 99-50-H.

503 Van Gosen BS, Fey DL, Shah AK, Verplanck PL, Hoefen TM (2014) Deposit model for heavy-
504 mineral sands in coastal environments. U.S. Geological Survey Scientific Investigations Report
505 2010-5070-L. doi:10.3133/sir20105070L.

506 Van Gosen BS, Bleiwas DI, Bedinger GM, Ellefsen KJ, Shah AK (2016) Coastal deposits of heavy
507 mineral sands: global significance and U.S. resources. Min Eng 68(10):36-43.

508 Verduzco B, Fairhead JD, Green CM, MacKenzie C (2004) New insights into magnetic derivatives
509 for structural mapping. Lead Edge 23:116-119. doi:10.1190/1.1651454.

510 Woodroffe CD (2000) Deltaic and estuarine environments and their Late Quaternary dynamics on
511 the Sunda and Sahul shelves. Journal of Asian Earth Sciences 18(4):393-413.
512 https://doi.org/10.1016/S1367-9120(99)00074-7.